MIP Reformulation for Max-min Problems in Two-stage Robust SCUC

Hongxing Ye, *Member, IEEE,* Jianhui Wang, *Senior Member, IEEE,* Zuyi Li, *Senior Member, IEEE*

***Abstract*—With increasing renewable penetration in power systems, a lot of research efforts have been focused on how to accommodate the uncertainties from renewables in the Security-Constraint Unit Commitment (SCUC) problem. One of the candidate approaches to handling uncertainties is the two-stage Robust SCUC (RSCUC), which enables system to survive in any scenario. The survivability is guaranteed by the solution optimality of the max-min problem in the second stage. However, as the non-convex max-min problem is NP-hard, it is difficult to get the exact optimal solution in acceptable time. In this paper, we propose a new efficient formulation which recasts the max-min problem to a Mixed Integer Programming (MIP) problem using Binary Expansion (BE). The upper bound of the gap between the new MIP problem and the original max-min problem is derived. The gap, which quantifies the solution optimality of the max-min problem, is controllable. Two effective acceleration techniques are proposed to improve the performance of the MIP problem by eliminating inactive flow constraints and decomposing time-coupled uncertainty budget constraints. Accordingly, the computation burden of solving the max-min problem is reduced tremendously. The simulation results for the IEEE 118-Bus system validate and demonstrate the effectiveness of the new BE-based solution approach to the two-stage RSCUC and the acceleration techniques.**

***Index Terms*—robust SCUC, max-min problem, renewables, binary expansion, line congestion**

I. Introduction

The Renewable Energy Sources (RES), such as wind and solar, have low production cost and are free of carbon emission. The penetration level of RES keeps climbing in recent decades, which helps lower the energy production cost and protect the environment. However, they also pose major challenges to electricity markets as the RES output cannot be predicted accurately in day ahead. In the U.S. Day-ahead Market (DAM), the Independent System Operator (ISO) or Regional Transmission Organization (RTO) performs the Security-Constraint Unit Commitment (SCUC) and Economic Dispatch (ED) to clear the market [1], [2]. In the SCUC and ED problem, the ISO/RTO determines the unit commitment (UC) and ED for the next day with lowest cost to supply the forecasted load while respecting a set of constraints. The system-wide constraints may include the load demand balance, transmission capacity limit, and reserve requirement. The unit-wise constraints are normally composed of generation capacity limits, ramping rate limits, and minimum on/off time limits [2], [3]. The uncertainties from RESs pose new challenges for the SCUC and ED problems in DAM, which have attracted extensive attention in recent years [4]–[13].

This work is supported in part by the U.S. National Science Foundation Grant ECCS-1549937. J. Wang's work is supported by the U.S. Department of Energy (DOE)'s Office of Electricity Delivery and Energy Reliability.
H. Ye and Z. Li are with the Robert W. Galvin Center for Electricity Innovation at Illinois Institute of Technology, Chicago, IL 60616, USA. (e-mail: hye9@hawk.iit.edu; lizu@iit.edu). J. Wang is with Argonne National Laboratory, Argonne, IL, USA (jianhui.wang@anl.gov).

The two-stage Robust SCUC (RSCUC) can accommodate any uncertainty in the second stage according to the re-dispatch process [8]–[10]. It exactly meets the reliability and security requirement which is the first priority in power system operation. Although the RSCUC is studied intensively, it has not been widely applied in the real markets. One of the reasons is that the max-min problem in the solution approach is NP-hard. It should be emphasized that the largest merit of RSCUC, robustness, is dependent on the optimality of the solution to the max-min problem. The max-min problem is often converted to a maximization problem according to the duality theory, which introduces bilinear terms in the new objective function. In the Extreme Point (EP) based solution approach, EPs are explicitly formulated for uncertainties to linearize the bilinear terms [8], [10]. However, the EP approach is dependent on the availability of the closed form of the EPs. It is also intractable when the number of the EPs is large. Researchers also employ Outer Approximation (OA) [9] and Mountain Climbing (MC) [11], [12], [14] to heuristically solve the max-min problem with good computation efficiency. However, the global optimality is not guaranteed in these approaches, which may lead to the *loss of robustness*. If KKT conditions are adopted [15], [16], a mathematical program with equilibrium constraints (MPEC) can be established. But MPEC is notoriously hard to solve in practice. An alternative way is to avoid the max-min problem. The affine policy (AP) as shown in [17] is successfully adopted in the literature [16], [18]–[20] with better computation performance. However, replacing the full recourse strategy with strict AP will further deteriorate the value of the robust solution, which is already criticized for over-conservatism.

In this paper, we propose to solve the max-min problem in an innovative way. Instead of enumerating the EPs of the uncertainty set, the bilinear terms in the objective function is linearized based on the Binary Expansion (BE) technique. The contributions of this paper are

1) The BE approach is proposed to recast the max-min problem in the robust optimization framework into a mixed-integer programming (MIP) problem. The BE solution approach does not rely on the closed form EPs of the uncertainty set. Hence, it is still applicable when it is hard to formulate the EPs. In particular, when sophisticated uncertainty sets are considered to relieve the conservativeness, the BE approach shows

more advantages over the EP approach.

2) A closed-form upper bound of the optimality gap in the BE approach is derived. It can be obtained directly without solving any optimization problem. Furthermore, the optimality gap can be adjusted by changing the number of BE terms. Accordingly, the solution quality of the max-min problem becomes observable and controllable.
3) Two acceleration techniques, bilinear term reduction and decomposition, are applied to reduce the solution time for the MIP problem in the BE approach. A generalized sufficient conditions for inactive line constraints in the max-min problem are derived and used to reduce most of the bilinear terms. By exploring the special structure of the max-min problem, the original time-coupled max-min problem is decomposed into smaller time-decoupled max-min problems. While the idea of the two acceleration techniques is not new, the combined use of the techniques along with the BE approach is novel and makes it much more efficient to solve the max-min subproblem, the most time-consuming step in the robust optimization framework.

In this paper, the matrix is denoted with bold uppercase letter, the vector with bold lowercase letter, and the scalar with normal font letter. The rest of this paper is organized as follows. In Section II. the RSCUC framework and the max-min problem are introduced. Then in Section III, the BE based approach to solving the max-min problem is proposed and the closed form of the optimality gap is derived. In Section IV, the two acceleration techniques to reduce the solution time are presented. The case studies are presented with the IEEE 118-Bus system in Section V. Finally, Section VI concludes this paper.

II. Two-stage Robust SCUC

A. Uncertainty Set

The uncertainties in the SCUC problem are mainly due to the forecasting errors for renewable power output and load. In the RSCUC literature [8], [9], these uncertainties are treated as load perturbation. The uncertainty set is modeled as

$$\begin{aligned}\mathcal{U} := \{(\boldsymbol{\epsilon_1}, \cdots, \boldsymbol{\epsilon_T}) \in \mathbb{R}^{N_d} \times \cdots \times \mathbb{R}^{N_d} :& \\ -\boldsymbol{u_t} \le \boldsymbol{\epsilon_t} \le \boldsymbol{u_t}, \forall t & \quad (1)\\ \boldsymbol{S_t \epsilon_t} \le \boldsymbol{h_t}, \forall t & \quad (2)\\ \sum_m \frac{|\epsilon_{m,t}|}{u_{m,t}} \le \Lambda_t, \forall t & \quad (3)\\ \sum_t \sum_m \frac{|\epsilon_{m,t}|}{u_{m,t}} \le \Lambda\}, & \quad (4)\end{aligned}$$

where N_d and T are the numbers of uncertain load injections and scheduling periods, respectively, and $\boldsymbol{\epsilon}_t$ represents the uncertainty vector at time t. $\epsilon_{m,t} \in \mathbb{R}$ is the entry in the vector $\boldsymbol{\epsilon}_t$. Define $\boldsymbol{\epsilon} = [\boldsymbol{\epsilon}_1^\top, \cdots, \boldsymbol{\epsilon}_T^\top]^\top$. The $\mathcal{U}$ defined in this paper combines the uncertainty set in [9]–[11]. Eq. (1) implies that the uncertainties are limited in intervals. The general polytope (2) can include many potential constraints. The single-hour budget constraint for uncertainties is formulated in (3). The time-coupled budget constraint is formulated in (4). The budget parameter Λ_t and Λ are assumed integers. By modeling constraints (2),(3),(4), the feasible region of $\mathcal{U}$ can be reduced. Consequently, the solution of the RSCUC will be less conservative.

B. Two-stage Robust RSCUC

This paper focuses on the solution approach for the max-min subproblem in RSCUC, We first briefly introduce a self-contained two-stage RSCUC model. The details can be found in [10], [16]. The RSCUC is formulated as

$$\begin{aligned}\text{(P)} \quad \min_{(\boldsymbol{x},\boldsymbol{p})\in\mathcal{F}} \quad & \mathcal{C}(\boldsymbol{x},\boldsymbol{p}) & (5)\\ \text{s.t.} \quad & \boldsymbol{Ax}+\boldsymbol{Bp} \le \boldsymbol{b} & (6)\end{aligned}$$

and

$$\begin{aligned}\mathcal{F} := \Big\{(\boldsymbol{x},\boldsymbol{p}) : \forall\boldsymbol{\epsilon}\in\mathcal{U}, \exists\boldsymbol{\Delta p} \text{ such that}&\\ \boldsymbol{D}(\boldsymbol{p}+\boldsymbol{\Delta p}) + \boldsymbol{E\epsilon} \le \boldsymbol{h} & \quad (7)\\ \boldsymbol{Fx}+\boldsymbol{Gp}+\boldsymbol{H\Delta p} \le \boldsymbol{g}\Big\}. & \quad (8)\end{aligned}$$

The objective (5) is to find the UC and ED solution with the least cost, which can be immunized against any realization of the uncertainty predefined in $\mathcal{U}$. Binary variable vector $\boldsymbol{x}$ denotes the UC variables. $\boldsymbol{p} \in \mathbb{R}^{N_G N_T}$ denotes the ED variables, respectively. N_G is the number of generators. $\boldsymbol{A}, \boldsymbol{B}, \boldsymbol{D}, \boldsymbol{E}, \boldsymbol{F}, \boldsymbol{G},$ and $\boldsymbol{H}$ are abstract matrices for representing constraints. Particularly, $\boldsymbol{E} \in \mathbb{R}^{N_s \times N_d N_T}$ where N_s is the number of rows in (7). Equation (6) represents UC and network constraint for the base-case scenario. $\boldsymbol{\Delta p} \in \mathbb{R}^{N_G N_T}$ stands for the generation adjustment for uncertainty accommodation. The re-dispatch process respects the system-wide constraints in (7) as well as the unit-wise constraint (8).

Similar to [10], the Column Generation (CG) in [15] is adopted to solve the RSCUC. The master problem (MP) and the subproblem (SP) are established as follows.

$$\begin{aligned}\text{(MP)} \quad & \min_{(\boldsymbol{x},\boldsymbol{p})} \quad \mathcal{C}(\boldsymbol{x},\boldsymbol{p}) &\\ \text{s.t.} \quad & \boldsymbol{Ax}+\boldsymbol{Bp} \le \boldsymbol{b} &\\ & \boldsymbol{D}(\boldsymbol{p}+\boldsymbol{\Delta p^w}) \le \boldsymbol{h} - \boldsymbol{E}\hat{\boldsymbol{\epsilon}}^{\boldsymbol{w}}, \forall w\in\mathcal{W} & (9a)\\ & \boldsymbol{Fx}+\boldsymbol{Gp}+\boldsymbol{H\Delta p^w} \le \boldsymbol{g}, \forall w\in\mathcal{W} & (9b)\end{aligned}$$

and

$$\text{(SP)} \qquad \phi := \max_{\boldsymbol{\epsilon}\in\mathcal{U}} \min_{(\boldsymbol{s},\boldsymbol{\Delta p})\in\mathcal{R}(\boldsymbol{\epsilon})} \boldsymbol{1}^\top \boldsymbol{s} \qquad (10a)$$

$$\begin{aligned}\mathcal{R}(\boldsymbol{\epsilon}) := \Big\{(\boldsymbol{s},\boldsymbol{\Delta p}) : \boldsymbol{s} \ge \boldsymbol{0} & \quad (10b)\\ \boldsymbol{D\Delta p} - \boldsymbol{s} \le \boldsymbol{h} - \boldsymbol{Dp} - \boldsymbol{E\epsilon} & \quad (10c)\\ \boldsymbol{H\Delta p} \le \boldsymbol{g} - \boldsymbol{Fx} - \boldsymbol{Gp}\Big\} & \quad (10d)\end{aligned}$$

where $\mathcal{W}$ is the index set for uncertainty points $\hat{\boldsymbol{\epsilon}}$ which are dynamically generated in (SP) during the solution procedure as described in Algorithm 1. The detailed formulation of $\mathcal{R}(\boldsymbol{\epsilon})$ can be found in Appendix A.

In fact, (MP) is similar to the scenario-based Stochastic SCUC (SSCUC). It is noted that both (MP) and (SP) are NP-hard problems [21], [22]. In particular, it is difficult to get the exact optimal solution to the max-min problem (SP).

Algorithm 1 Column Generation Procedure to Solve (P)

$\mathcal{W} \leftarrow \emptyset, w \leftarrow 1, \phi \leftarrow +\infty$, define feasibility tolerance δ
while $\phi \geq \delta$ **do**
  Solve (MP), obtain optimal $(\hat{\boldsymbol{x}}, \hat{\boldsymbol{p}})$.
  Solve (SP) with $\boldsymbol{x} = \hat{\boldsymbol{x}}, \boldsymbol{p} = \hat{\boldsymbol{p}}$, get solution $(\phi, \hat{\boldsymbol{\epsilon}}^{\boldsymbol{w}})$
  $\mathcal{W} \leftarrow \mathcal{W} \cup w, w \leftarrow w + 1$
end while

III. A MIP Reformulation for Max-min Problem

The max-min problem (SP) is converted to a maximization problem based on duality theory [8], [9], [16]. The converted bilinear maximization problem (BP) is formulated as

$$\text{(BP)} \quad \phi = \max_{\boldsymbol{\epsilon} \in \mathcal{U}, \boldsymbol{\lambda}, \boldsymbol{\mu}} \quad -\boldsymbol{\lambda}^\top \tilde{\boldsymbol{h}} + \boldsymbol{\lambda}^\top \boldsymbol{E} \boldsymbol{\epsilon} - \boldsymbol{\mu}^\top \tilde{\boldsymbol{g}} \tag{11}$$

$$\text{s.t.} \quad \boldsymbol{D}^\top \boldsymbol{\lambda} + \boldsymbol{H}^\top \boldsymbol{\mu} = \boldsymbol{0} \tag{12}$$

$$\boldsymbol{0} \leq \boldsymbol{\lambda} \leq \boldsymbol{1}, \quad \boldsymbol{\mu} \geq \boldsymbol{0}, \tag{13}$$

where $\tilde{\boldsymbol{h}} := \boldsymbol{h} - \boldsymbol{D}\boldsymbol{p}$ and $\tilde{\boldsymbol{g}} := \boldsymbol{g} - \boldsymbol{F}\boldsymbol{x} - \boldsymbol{G}\boldsymbol{p}$. Due to the quadratic term $\boldsymbol{\lambda}^\top \boldsymbol{E}\boldsymbol{\epsilon}$ in the objective function (11), (BP) is hard to solve.

In this paper, the Binary Expansion (BE) is used to linearize the bilinear term $\boldsymbol{\lambda}^\top \boldsymbol{E}\boldsymbol{\epsilon}$ [23]. The basic idea of the BE is originated from the conversion from a decimal number to a binary number. An integer in the decimal number system can be equivalently converted to a number in the binary number system. Consider an entry λ_i in vector $\boldsymbol{\lambda}$. As $\lambda_i \in [0, 1]$,

$$2^K \lambda_i \approx \sum_{k'=0}^{K} 2^{k'} z_{i,k'},$$

where K is an integer and $z_{i,k} \in \{0, 1\}, \forall k$. Hence, we get

$$\begin{cases} \lambda_i \approx \sum_{k=0}^{K} 2^{-k} z_{i,k}, \forall i, & (14) \\ z_{i,k} \in \{0, 1\}, \forall i, k. & (15) \end{cases}$$

With the BE technique, we have the following theorem to solve (BP).

Theorem 1. Introduce auxiliary parameter $\underline{\boldsymbol{q}} \in \mathbb{R}^{N_s}, \bar{\boldsymbol{q}} \in \mathbb{R}^{N_s}$,

$$\underline{q}_i = \min_{\boldsymbol{\epsilon} \in \mathcal{U}} \boldsymbol{E_i} \boldsymbol{\epsilon}, \quad \bar{q}_i = \max_{\boldsymbol{\epsilon} \in \mathcal{U}} \boldsymbol{E_i} \boldsymbol{\epsilon} - \underline{q}_i. \tag{16}$$

The problem (BP) is approximated as

$$\text{(RP)} \; \phi^a(K) = \max_{\boldsymbol{\epsilon} \in \mathcal{U}, \lambda, \mu} \sum_{i}^{N_s} \sum_{k=0}^{K} 2^{-k} \xi_{i,k} + \boldsymbol{\lambda}^\top (\underline{\boldsymbol{q}} - \tilde{\boldsymbol{h}}) - \boldsymbol{\mu}^\top \tilde{\boldsymbol{g}}$$

$$\text{s.t.} \quad \boldsymbol{D}^\top \boldsymbol{\lambda} + \boldsymbol{H}^\top \boldsymbol{\mu} = \boldsymbol{0}$$

$$\sum_{k=0}^{K} 2^{-k} z_{i,k} \leq \lambda_i \leq \sum_{k=0}^{K} 2^{-k} z_{i,k} + 2^{-K} \tag{17}$$

$$\boldsymbol{q} = \boldsymbol{E}\boldsymbol{\epsilon} - \underline{\boldsymbol{q}} \tag{18}$$

$$\boldsymbol{0} \leq \boldsymbol{\lambda} \leq \boldsymbol{1}, \quad \boldsymbol{\mu} \geq \boldsymbol{0}$$

$$\xi_{i,k} \leq q_i, \quad \xi_{i,k} \leq \bar{q}_i z_{i,k}, \quad \forall i, k$$

$$z_{i,k} \in \{0, 1\}, \forall i, k,$$

where K is a given integer.

The proof of Theorem 1 is given in Appendix B. $\boldsymbol{E_i}$ denotes the i^{th} row in $\boldsymbol{E}$. Theorem 1 presents an alternative method to the solution of the bilinear problem. Notice a relaxed $\mathcal{U}$ in (16) is the box constraint (1). In this case, the *closed forms* of $\underline{\boldsymbol{q}}$ and $\bar{\boldsymbol{q}}$ are available and all the principles are still applicable. The closed forms are

$$\underline{q}_i = \boldsymbol{E_i^-} \boldsymbol{u} - \boldsymbol{E_i^+} \boldsymbol{u}, \quad \bar{q}_i = 2\boldsymbol{E_i^+} \boldsymbol{u} - 2\boldsymbol{E_i^-} \boldsymbol{u}, \tag{19}$$

where $\boldsymbol{u}$ is the non-negative bound vector of the uncertainty. $\boldsymbol{E_i^-}$ and $\boldsymbol{E_i^+}$ are

$$\boldsymbol{E_i^-} = \Big(\boldsymbol{E_i} - \text{abs}(\boldsymbol{E_i})\Big)/2, \quad \boldsymbol{E_i^+} = \Big(\boldsymbol{E_i} + \text{abs}(\boldsymbol{E_i})\Big)/2,$$

where abs$(\bullet)$ is a vector whose elements are the absolute values of the elements in $\bullet$. The process of determining of $\bar{\boldsymbol{q}}$ and $\underline{\boldsymbol{q}}$ is as follows.

Formulate matrix $\boldsymbol{E}$.
for $i = 1$ **to** N_s **do**
  Generate $\boldsymbol{E}_i^+$ and $\boldsymbol{E}_i^-$
  Get $\bar{q}_i$ and $\underline{q}_i$ according to (19)
end for

We have the following theorem regarding the solution quality.

Theorem 2. The gap between problem (BP) and (RP) follows

$$|\phi - \phi^a(K)| \leq 2^{-K} \sum_{i}^{N_s} \bar{q}_i, \tag{20}$$

where ϕ is the optimal value to (BP) and $\phi^a(K)$ is the optimal value to (RP) given K.

The proof of Theorem 2 is given in Appendix B. Theorem 2 shows that the solution quality, which is represented by the gap, is *observable and controllable*. The gap is observable as it is always smaller than $2^{-K} \sum_i^{N_s} \bar{q}_i$. The upper bound in Theorem 2 can be determined directly by (19) without solving (RP) or (BP). The gap is controllable as it can be adjusted by the parameter K. By increasing K, the gap can be lowered. Based on Theorem 1 and 2, (BP) can be approximately solved by (RP) with a controllable gap. Compared to the EP approach [8], the BE approach can also handle other uncertainty sets whose EPs are hard to model or even do not exist. In fact, the MC and OA approaches can also approximately solve (BP) [9], [11]. A major advantage of the EP approach is that its solution quality is observable and controllable while the optimality of MC and OA approach is unknown.

IV. Acceleration Techniques

The large number of rows in $\boldsymbol{E}$ leads to heavy computation burden in the MIP problem (RP). In this section, two effective acceleration techniques are proposed to reduce the computation burden. The first acceleration technique, which is also applicable to other approaches, is derived based on a sufficient condition to reduce inactive network constraints. The second technique is proposed by exploring the special structure of the max-min problem. We decompose the original time-coupled max-min problem into smaller time-decoupled problems at each hour.

A. Reduction of Bilinear Terms

The bilinear term $\boldsymbol{\lambda}^\top \boldsymbol{E}\boldsymbol{\epsilon}$ is derived from the load balance constraints and network capacity limits. If the number of transmission lines is N_L, then there are $2 \times N_L \times N_T$ line constraints modeled in the max-min problem. Consequently, these system-wide constraints lead to a large number of integer variables, which increases the problem size of (RP). Next, we show that only part of them will remain after the reduction of bilinear terms based on the sufficient conditions for inactive constraints.

The strategy is to identify the inactive line constraints and eliminate them from (SP). However, the identification is made more complicated due to the slack variables in $\mathcal{R}(\boldsymbol{\epsilon})$. The non-negative s in (44) in Appendix A may cause a large number of line constraints in (SP) to become non-redundant. In order to address this issue, consider

$$\begin{aligned}\mathcal{R}'(\boldsymbol{\epsilon}) := \Big\{(\boldsymbol{\Delta p}, \boldsymbol{s^{L+}}, \boldsymbol{s^{L-}}) : \boldsymbol{s^{L+}}, \boldsymbol{s^{L-}} \geq \boldsymbol{0},\\ \sum_g (p_{g,t} + \Delta p_{g,t}) = \sum_m (d_{m,t} + \epsilon_{m,t}), \forall t \quad (21)\\ (45), (46), (47)\Big\}.\end{aligned}$$

Compared to $\mathcal{R}(\boldsymbol{\epsilon})$ in Appendix A, (21) does not include slack variables in the load balance constraint. Then a new subproblem (USP)

$$\text{(USP)}\ \phi^u := \max_{\boldsymbol{\epsilon}\in\mathcal{U}} \min_{(\boldsymbol{s},\boldsymbol{\Delta p})\in\mathcal{R}'(\boldsymbol{\epsilon})} \boldsymbol{1}^\top \boldsymbol{s} \tag{22}$$

can be formulated. As there is no slack variable in (21), the following sufficient conditions are established to identify the inactive line constraints based on [24].

Theorem 3. Consider the net power injection $p^{\text{inj}}_{m,t} \in [\underline{p}^{\text{inj}}_{m,t}, \bar{p}^{\text{inj}}_{m,t}]$ on bus m at time t, and introduce auxiliary variable $p^{\text{inj}+}_{m,t} = p^{\text{inj}}_{m,t} - \underline{p}^{\text{inj}}_{m,t}$

$$0 \leq p^{\text{inj}+}_{m,t} \leq \bar{p}^{\text{inj}+}_{m,t} = \bar{p}^{\text{inj}}_{m,t} - \underline{p}^{\text{inj}}_{m,t}, \forall m, t. \tag{23}$$

Denote $p^{\text{vt}}_t = -\sum_m \underline{p}^{\text{inj}}_{m,t}$, and $f^{\text{vt}}_{l,t} = \sum_{m=1}^{N_d} \Gamma_{l,m}\underline{p}^{\text{inj}}_{m,t}$. If there exists an integer $j \in [1, N_d]$ so that

$$\begin{cases} \sum_{n=1}^{j-1} \bar{p}^{\text{inj}+}_{m_n,t} \leq p^{\text{vt}}_t \leq \sum_{n=1}^{j} \bar{p}^{\text{inj}+}_{m_n} & (24)\\ \sum_{n=1}^{j-1} (\Gamma_{l,m_n} - \Gamma_{l,m_j})\bar{p}^{\text{inj}+}_{m_n,t} + \Gamma_{l,m_j} p^{\text{vt}}_t + f^{\text{vt}}_{l,t} \leq F_l & (25)\\ \Gamma_{l,m_1} \geq \Gamma_{l,m_2} \geq \cdots \geq \Gamma_{l,m_{N_d}} & (26)\end{cases}$$

holds, then the flow constraint for line l (with a capacity of F_l) in the positive direction at t is inactive. m_n is the bus with the n^{th} largest shift factor Γ_{l,m_n} for line l.

The proof of Theorem 3 is shown in Appendix C. Theorem 3 is a generalized and extended work inspired by [25]. The main differences are that Theorem 3 is established for max-min problems considering uncertainties and it can be applied to other bi-level problems. In [25], the search for the upper/lower bound of the power flow is finished when the sum of the generator capacities is larger than the constant load demand.

Algorithm 2 Solve (P) with Elimination Techniques

1: $\mathcal{W} \leftarrow \emptyset, w \leftarrow 1, \phi \leftarrow +\infty$, define feasibility tolerance δ
2: **while** $\phi \geq \delta$ **do**
3: Solve (MP), obtain optimal $(\hat{\boldsymbol{x}}, \hat{\boldsymbol{p}})$.
4: Update matrix $\boldsymbol{E}$ by applying conditions in Theorem 3
5: Solve (RP) with $\boldsymbol{x} = \hat{\boldsymbol{x}}, \boldsymbol{p} = \hat{\boldsymbol{p}}$, get solution $(\phi, \hat{\boldsymbol{\epsilon}}^w)$
6: $\mathcal{W} \leftarrow \mathcal{W} \cup w, w \leftarrow w + 1$
7: **end while**

In the max-min problem, the load demand is not constant anymore. Instead, it is a variable. In Theorem 3, a key task is to find the tight enough lower and upper bounds for net power injection. Fortunately, given $\boldsymbol{p}$, the closed forms of $\bar{p}^{\text{inj}}_{m,t}$ and $\underline{p}^{\text{inj}}_{m,t}$ can be obtained according to ramping limits and generation capacities that limit $\boldsymbol{\Delta p}$ and the box constraint for $\boldsymbol{\epsilon}$. They are

$$\begin{cases} \bar{p}^{\text{inj}}_{m,t} = \sum_{g\in\mathcal{G}(m)} \Big(p_{g,t} + \bar{r}_{g,t}(\boldsymbol{x}, \boldsymbol{p})\Big) - d_{m,t} + u_{m,t}, \forall m, t\\ \underline{p}^{\text{inj}}_{m,t} = \sum_{g\in\mathcal{G}(m)} \Big(p_{g,t} + \underline{r}_{g,t}(\boldsymbol{x}, \boldsymbol{p})\Big) - d_{m,t} - u_{m,t}, \forall m, t\end{cases}$$

where $\bar{r}_{g,t}(\boldsymbol{x}, \boldsymbol{p})$ and $\underline{r}_{g,t}(\boldsymbol{x}, \boldsymbol{p})$ are the upper bound and lower bound of $\Delta p_{g,t}$. They are the functions of given UC and ED as well as unit ramping rates and generation capacities.

By applying Theorem 3, matrix $\boldsymbol{E}$ can be significantly reduced. Consequently, unnecessary binary decision variables and constraints in (RP) are also eliminated. Once the shift factors are ordered, the computation complexity is $O(N_d)$ in Theorem 3. The new procedure to solve (P) is presented in Algorithm 2.

The expense of replacing $\mathcal{R}$ with $\mathcal{R}'$ is that the dual variables for load balance constraints become unbounded. However, in Algorithm 2, $\boldsymbol{0} \leq \boldsymbol{\lambda} \leq \boldsymbol{1}$ is still used in (RP). The following proposition shows that it will not alter the converged solution to (P).

Proposition 1. The optimal value ϕ^u to (USP) is an upper bound of the optimal value ϕ to (SP) or (BP), i.e. $\phi^u \geq \phi$. Given the optimal $(\boldsymbol{x}^*, \boldsymbol{p}^*)$ to (P), then $\phi^u = \phi$, and optimal solution $(\boldsymbol{\lambda}^*, \boldsymbol{\mu}^*)$ to (BP) is also the optimal dual variables to the inner-level minimization problem in (USP).

The proof of Proposition 1 is given in Appendix E. Proposition 1 shows that if the procedure in Algorithm 2 has not converged at iteration w, $\hat{\boldsymbol{\epsilon}}^w$ may not be the worst point. Fortunately, $\hat{\boldsymbol{\epsilon}}^w$ is guaranteed to be the worst point if the procedure converges at iteration w. Therefore, the robustness is also guaranteed. Accordingly, (25) can be replaced with

$$\sum_{n=1}^{j-1} (\Gamma_{l,m_n} - \Gamma_{l,m_j})\bar{p}^{\text{inj}+}_{m_n,t} + \Gamma_{l,m_1}\delta + \Gamma_{l,m_j} p^{\text{vt}}_t + f^{\text{vt}}_{l,t} \leq F_l \tag{27}$$

in Theorem 3 when feasibility tolerance δ, which is a metric for the solution robustness, is considered.

The BE and inactive constraint identification contribute to the performance improvement together. In the proposed BE approach, the inactive constraint identification helps eliminate the bilinear terms whose optimal values are zero. Consequently, the number of binary variables and related constraints are dramatically reduced in (RP), and the performance is improved.

B. Decomposition of Time-coupled Budget Constraints

In this subsection, a model dependent decomposition technique is proposed by exploring the special structure of (SP). As $(\boldsymbol{x}, \boldsymbol{p})$ is given in the master problem, the re-dispatch variable $\boldsymbol{\Delta p}$ and slack variable $\boldsymbol{s}$ are time decoupled. The only time-coupled variable is $\boldsymbol{\epsilon}$ due to the constraints (4). In the following, a technique is proposed to handle the time-coupled budget constraints. We illustrate the technique with (SP), which is also applicable in Algorithm 2.

Consider an uncertainty set at hour t

$$\mathcal{V}_t(v_t) := \Big\{ \boldsymbol{\epsilon}_t \in \mathbb{R}^{N_d} : (1), (2), \sum_m \frac{|\epsilon_{m,t}|}{u_{m,t}} \le v_t \Big\}. \tag{28}$$

Then a new max-min problem at hour t can be formulated as

$$\phi_t(v_t) := \max_{\boldsymbol{\epsilon}_t \in \mathcal{V}_t(v_t)} \min_{(\boldsymbol{s}_t, \hat{\boldsymbol{p}}_t) \in \mathcal{R}_t(\boldsymbol{\epsilon})} \mathbf{1}^\top \boldsymbol{s}_t \tag{29a}$$

$$\mathcal{R}_t(\boldsymbol{\epsilon}) := \Big\{ (\boldsymbol{s}_t, \boldsymbol{\Delta p}_t) : \boldsymbol{s}_t \ge \mathbf{0} \tag{29b}$$

$$\boldsymbol{D}_t \boldsymbol{\Delta p}_t - \boldsymbol{s}_t \le \boldsymbol{h}_t - \boldsymbol{D}_t \boldsymbol{p}_t - \boldsymbol{E}_t \boldsymbol{\epsilon}_t \tag{29c}$$

$$\boldsymbol{H}_t \boldsymbol{\Delta p}_t \le \boldsymbol{g}_t - \boldsymbol{F}_t \boldsymbol{x}_t - \boldsymbol{G}_t \boldsymbol{p}_t \Big\} \tag{29d}$$

where subscript t denotes the parameters or variables associated with hour t. It is observed that budget parameter v_t is used in the above max-min problem. We have the following proposition regarding v_t and the solution to (SP).

Proposition 2. Consider the problem

$$\text{(IP)}: \quad \phi^{\text{IP}} := \max_{v_t, \forall t} \sum_t \phi_t(v_t) \tag{30}$$

$$\text{s.t.} \quad \sum_t v_t \le \Lambda, v_t \le \Lambda_t, v_t \in \mathbb{Z}_+, \tag{31}$$

$\phi^{\text{IP}} = \phi$ holds. Denote the optimal solution to (IP) as $v_t^*, \forall t$. Given v_t^*, the solution $\boldsymbol{\epsilon}_t(v_t^*)$ to problem (29a) is a sub-vector of optimal solution $\boldsymbol{\epsilon}^*$ to problem (SP) at t.

The proof of Proposition 2 is given in Appendix 2. With the values $\phi_t(v_t)$ obtained by solving (29a), (IP) can be casted as an MIP problem or simply an ordering problem, which can be solved efficiently. In fact, all the subproblems (29a) with different v_t at various time intervals can be solved *in parallel*. Moreover, we also design an efficient sequential algorithm to solve the problem (IP). It is presented in Algorithm 3. Its computation complexity is analyzed by counting the max-min subproblems as follows.

Theorem 4. There are at most $2T + \sum_t \Lambda_t - \Lambda$ max-min problem (29a) to be solved.

Algorithm 3 Algorithm to Solve Problem (IP)

$\phi^{\text{IP}} \leftarrow 0$
for $t = 1$ **to** T **do**
  Solve (29a) with $v_t = \Lambda_t$
  $\phi^{\text{IP}} \leftarrow \phi^{\text{IP}} + \phi_t(v_t)$
end for
while $\sum_t v_t > \Lambda$ **do**
  for $t = 1$ **to** T **do**
    if $\phi_t - 1 \ge 0$ **and** $\phi_t(v_t - 1)$ is not available **then**
      Calculate $\phi_t(v_t - 1)$ by solving (29a)
      $\Delta_t = \phi_t(v_t) - \phi_t(v_t - 1)$
    end if
  end for
  $v_t \leftarrow v_t - 1$, where t is the index of the minimum one with $v_t \ge 1$ in $\{\Delta_1, \cdots, \Delta_T\}$
  $\phi^{\text{IP}} \leftarrow \phi^{\text{IP}} - \Delta_t$
end while

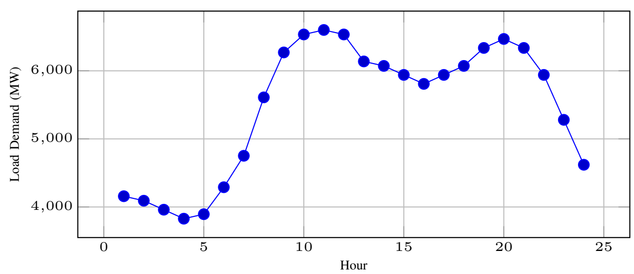

Fig. 1. Load Demand Profile in 24 Hours

V. Case Study

The proposed solution approach to solve the max-min problem is tested in the IEEE 118-Bus system (http://motor.ece.iit.edu/Data/ROSCUC_118.xls). The experiments are performed on PC with Intel i7-3770@3.40GHz. Gurobi 5.6.3 is utilized to solve the MIP problem [26]. The MIPGap is set as 0.001 and TimeLimit is set as 400 seconds for Gurobi. The system consists of 54 units and 186 transmission lines. The load profile is illustrated in Fig. 1. It is assumed that uncertainties exist at 50 buses. $u_{m,t}$, an entry in $\boldsymbol{u}_t$, is set as 10% of the load at bus m. Three groups of case studies are performed.

1) We validate the effectiveness of the proposed BE approach in handling a group of uncertainty sets.
2) We compare the computation performance and solution quality of the proposed BE approach with those of the EP approach [8], [10] and MC approach [11], [12].
3) We demonstrate the performance of the proposed acceleration techniques.

A. Effectiveness Validation of BE Approach

The IEEE 118-bus system is composed of 3 zones. The bus set in each zone is denoted as $\mathcal{Z}_n$. In this subsection, we assume the total uncertainties in a zone respects

$$L_{n,t}^z \le \sum_{m \in \mathcal{Z}_n} \epsilon_{m,t} \le U_{n,t}^z, \forall n, t. \tag{32}$$

TABLE I
OPTIMALITY GAPS V.S. INCREASING K

K	Gap (MW)	VioWorst (MW)	AverageCPUTimeRP (s)
10	18	0.078	9.1
20	0.018	0.0	27.6
30	0.000018	0.0	31.9

$\alpha = 1, \Lambda_t = 30, \Lambda = 720$

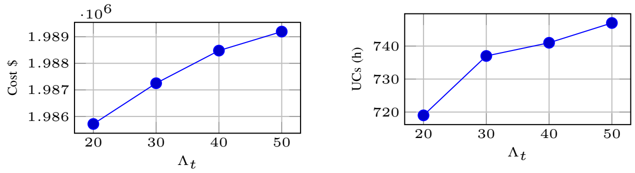

(a) Operation Cost (b) UC Hours

Fig. 2. Operation Cost and UCs v.s. Λ_t ($\alpha = 1, \Lambda = \sum_t \Lambda_t, K = 20$)

For simplicity, $L^z_{n,t}$ and $U^z_{n,t}$ are parameterized with α, i.e. $L^z_{n,t} = -\alpha \sum_{m \in \mathcal{Z}_n} u_{m,t}$ and $U^z_{n,t} = \alpha \sum_{m \in \mathcal{Z}_n} u_{m,t}$. If $\alpha = 1$, then (32) becomes inactive. It is noted that constraint (2) is general enough to model other linear constraints.

The procedure presented in Algorithm 2 converges in 8 iterations. The simulation results with different budget parameters Λ_t are shown in Fig. 2. The curve for the base-case cost is drawn with respect to different Λ_t in Fig. 2a. It is observed that the base-case cost is also low when Λ_t is small. With the increase of Λ_t, the base case cost is also ramping up. The UC hours, the sum of all committed unit hours, are depicted in Fig. 2b. When $\Lambda_t = 20$, around 720 UC hours are scheduled. The largest UC hours (around 748) happens when Λ_t is 50. It indicates that when the budget parameter is large, more reserves are required to maintain the solution robustness.

Fig. 3 presents the simulations with different α. Parameter α reflects the zonal confidence level for the uncertainty. The time-coupled budget parameter Λ is also set to 360. It can be observed that the base-case cost increases monotonically with α. When $\alpha = 0.2$, the cost is the lowest (around \$1,982,000). When $\alpha = 0.8$, the cost increases to around \$1,986,000. The UC hours depicted in Fig. 3b show a similar trend with α.

In fact, when the parameter Λ_t or α increases, the uncertainty set $\mathcal{U}$ is also enlarged. The experiments show that a larger uncertainty set leads to a more conservative solution to RSCUC in terms of the base-case costs and UC hours. Note that adding stronger constraints based on the historical data in $\mathcal{U}$ is preferred in RSCUC to reduce the conservativeness. The BE approach does not rely on the EPs of $\mathcal{U}$ to add constraints, which is one advantage of the BE approach over the EP approach.

Table I shows how the optimality gap is controlled by K based on Theorem 2. The upper bound of the gap, "Gap", decreases with K. The computation burden "AverageCPUTimeRP", which is the average CPU time of solving (RP) when the reduction technique is applied, normally increases with K in Gurobi. Column "VioWorst" shows the constraint violation in the worst-case scenario. It can be observed that the actual violation is much smaller than the upper bound of the gap.

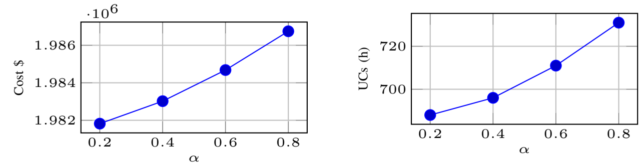

(a) Operation Cost (b) UC Hours

Fig. 3. Operation Cost and UCs v.s. α ($\Lambda_t = 30, \Lambda = 360, K = 20$)

TABLE II
BE V.S. MC AND EP

Approach	BaseCost (\$)	VioWorst (MW)	TotalCPUTime (s)
BE	1,987,255	0.0	144
MC	1,987,041	35	40
EP	1,987,250	0.0	2,653

$\alpha = 1, \Lambda_t = 30, \Lambda = 600, K = 20$

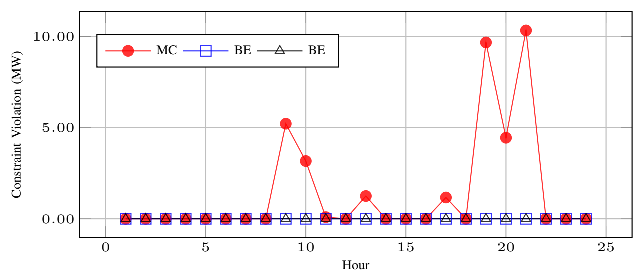

Fig. 4. Constraint Violation in the Worst Scenario ($\alpha = 1$)

B. Comparison with Other Approaches

In this part, the solution quality and performance of the BE approach are compared with those of the EP approach and MC approach [11], [12]. The optimality gap of the max-min problem is in fact also the solution robustness of the solution to RSCUC. The advantage of the MC approach is that only LP problems are solved to find the solution to the max-min problem. However, the solution is only locally optimal. In contrast, the EP approach and the BE approach can find the "globally" optimal solution with a known gap. We set the feasibility tolerance or the robustness tolerance $\delta = 0.01$ and the parameter used to control the optimality of the BE approach $K = 20$. Two cases are simulated for the three solution approaches, with the acceleration techniques in Section IV-A applied in all three approaches.

1) $\alpha = 1$. Constraint (32) becomes inactive. All three solution approaches are tested.
2) $\alpha = 0.5$. It becomes more complicated for the EP approach to handle the uncertainty set. For simplicity, only the BE approach and MC approach are tested.

1) $\alpha = 1$: Table II shows the experiment results. "BaseCost" shows the base-case cost. It can be observed that the optimal value obtained by the BE or EP approach is around \$214 higher than that obtained by the MC approach. In terms of the base-case cost, it seems that the solution from the MC approach is better than those from the BE or EP approach. However, the fact is that some worst points are missed in the MC approach, as shown in column "VioWorst", which represents the constraint violation in the worst-case scenario.

TABLE III
BE V.S. MC

Approach	BaseCost ($)	VioWorst (MW)	TotalCPUTime (s)
BE	1,983,823	0.0	61
MC	1,983,444	62	14

$\alpha = 0.5, \Lambda_t = 30, \Lambda = 600, K = 20$

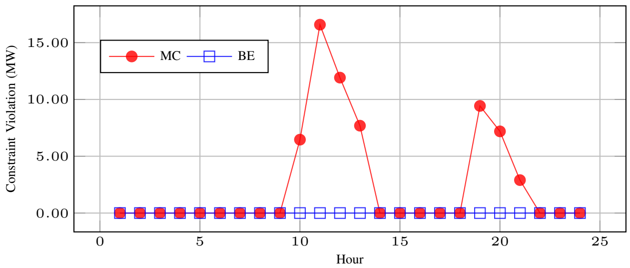

Fig. 5. Constraint Violation in the Worst Scenario ($\alpha = 0.5$)

The value in "VioWorst" is obtained by solving another max-min problem using the EP approach given the UC and ED solutions from the BE and MC approach. It is observed that the solution from the MC approach is not robust. In the worst-case scenario, the constraint violation is 35MW. The detailed values for the hourly constraint violations are depicted in Fig. 4. Fig. 4 shows that the constraint violations occur at Hour 9, 10, 13, 17, 19, 20, and 21. The largest violation 10MW happens at Hour 21. The total solution time for RSCUC in column "TotalCPUTime" verifies the computational advantage of the MC approach. The EP approach has the largest computation burden although its solution is exact. It should be pointed out that the computation burden of the EP approach is related to the number of the EPs. When there are only 30 buses with uncertainties in the system, the EP approach can find the solution in less than 200 seconds. In the EP approach, Theorem 3 eliminates the redundant constraints, but the number of the binary variables remains the same after the elimination. In the BE approach, Theorem 3 reduces the binary variables and eliminates the related constraints. The proposed BE approach shows a good trade-off between the robustness and the computation burden according to the data in Table II.

2) $\alpha = 0.5$: Table III and Fig. 5 depict the simulation results. Compared with the uncertainty set when $\alpha = 1$, the size of the uncertainty set in this part is reduced. Therefore, the base-case costs in Table III are lower than those in Table II. It can also be observed in Table III that the base-case cost obtained from the BE approach is higher than that from the MC approach, although the difference ($\$379 = 1,983,823 - 1,983,444$) is relatively small. However, the data in "VioWorst" shows that the BE approach is much better than the MC approach in terms of solution robustness. In the worst-case scenario, the total constraint violation of the MC approach is about 62MW. It is observed that the constraint violations are large at Hour 10-13, and 19-21, when the load demands are high.

The data in Table II and Table III show that the solution robustnesses can be significantly different even if the operation costs are close. This indicates the criticality of the solution

TABLE IV
ACCELERATION PERFORMANCE

Decomposition	Reduction	TotalCPUTime (s)	Obj ($)
No	No	NaN	NaN
Yes	No	4,799	1,983,909
No	Yes	197	1,983,879
Yes	Yes	61	1,983,823

$\alpha = 0.5, \Lambda_t = 30, \Lambda = 600, K = 20$

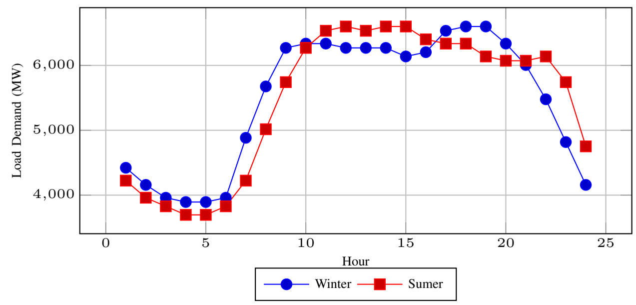

Fig. 6. Additional Load Demand Profiles in 24 Hours

optimality of the max-min problem. The fact that the solution from the MC approach fails to survive in the worst-case scenario is also consistent with the analysis in the first paragraph in this subsection.

C. Performance of Reformulation and Acceleration

In this part, we present the performance of the proposed reformulation and the two acceleration techniques introduced in Section IV. For the IEEE 118-bus system, there are $8,928 = 186 \times 2 \times 24$ network constraints and 24 equality constraints for load balance. When K is set as 20, we need to model $179,040$ binary variable z in the original (RP) shown in Section III. The decomposition technique in Section IV-B breaks the single time-coupled large max-min problem into a series of smaller problems, one for each time interval. Theorem 3 can remove about 95% inactive network constraints in the inner minimization problem of the max-min problem.

Table IV shows the different computation performances when we apply the acceleration techniques. Column "TotalCPUTime" presents the total CPU time when the procedure is converged. Column "Obj" shows the base-case operation cost. There are small cost differences, which are within \$100. It can be observed that no solution is found within the given time limit if we do not apply any acceleration techniques. Specifically, the MIP solver cannot get any feasible solution to problem (RP) within 400 seconds. With the decomposition technique only, the solution is found in 4,799 seconds after solving multiple MIP problems. With the reduction technique only, the solution time is reduced significantly to 197 seconds. The best performance (a solution time of 61 seconds) is achieved while applying both acceleration techniques. It is observed that in the max-min problem, the network constraint is the main factor leading to computation complexity.

The computational complexity is also dependent on the load profiles. Hence, additional simulations are performed with winter and summer load profiles from https://www.ee.

TABLE VI
NUMERICAL INFORMATION FOR THE MIP MODELS

Decomposition	Reduction	BE			BE (Presolved)			EP (Presolved)		
		# of Cons.	# of Var.	# of Bin.	# of Cons.	# of Var.	# of Bin.	# of Cons.	# of Var.	# of Bin.
No	No	389,160	381,696	178,080	345,974	345,879	162,816	9,744	19,222	2,400
Yes	No	16,215	15,904	7,420	14,401	14,398	6,784	406	764	100
No	Yes	10,803	20,937	2,100	7,324	7,279	2,019	9,276	10,026	2,400
Yes	Yes	606	1,021	160	457	454	153	403	486	100

# of Cons. : Number of Constraints;
# of Var. : Number of Continuous Variables and Binary Variables;
# of Bin. : Number of Binary Variables.

TABLE V
AVERAGE CPU TIME OF SOLVING ONE MAX-MIN PROBLEM

Decomposition	Reduction	Winter Profile		Summer Profile	
		BE (s)	EP (s)	BE (s)	EP (s)
No	No	2912	3600	1215	3600
Yes	No	40.1	3562	31.5	3600
No	Yes	13.2	3575	10.68	3600
Yes	Yes	0.71	304.10	0.62	512.32

$\alpha = 1, \Lambda_t = 30, \Lambda = 720, K = 20$

washington.edu/research/pstca/rts/rts96/Table-04.txt. The load curves are illustrated in Fig. 6. The TimeLimit for Gurobi is changed to 3600 seconds. Table V presents the average CPU time of solving one max-min problem. Theorem 3 can still eliminate over 95% line constraints. The solution process generally converges after up to 5 iterations using Algorithm 2, and in each iteration either one multi-period max-min problem or multiple single-period max-min problems should be solved.

In general, the CPU time has the same trend in the winter and summer load profiles. Table V shows that it is the most efficient to solve the single-period max-min problem with the reduction technique. In the BE approach, the average computation time is less than one second. With the reduction technique, the BE approach can also solve the multi-period max-min problem within 14 seconds on average. It is observed that applying decomposition technique leads to slightly longer average solution time in each iteration with the winter profile, i.e. $0.71 \times 24 = 17.04 > 13.2$. The bottom line is that it provides an option for the high-performance parallel computing, which is especially important when the size of the NP-hard problem is large. In the EP approach, the MIP solver often stops when the time limit is reached. The EP approach has much heavier computational burden than the BE approach according to Table V. In the winter case, the average CPU time is 304.1 seconds for solving a single-period max-min problem in the EP approach. It is 434 times that in the BE approach. In summary, the data in Table V suggests that the BE approach becomes powerful with the acceleration techniques. It also indicates that the acceleration techniques are more useful in the BE approach.

Table VI shows the numerical information for the typical MIP models in the two approaches. The Gurobi MIP solver can reduce the problem size by presolving the MIP problem. The information of the presolved model is also listed in the column "BE (Presolved)" and "EP (Presolved)". It can be observed that 178,080 variables are originally modeled in the BE approach. It is noted that 178,080 is smaller than $179,040 = (186 \times 2 + 1) \times 24$. The reason is that the shift factors for one line are all zeros with respect to the buses with uncertainties. In the presolved model, the number of binary variables is reduced by $15,264 = 178,080 - 162,816$ and the number of constraints is reduced by $43,186 = 389,160 - 345,974$. The decomposition technique alone can reduce the number of binary variables to 4.17% (i.e. 4.17%=6,784/162,816). The reduction technique alone can reduce the number of binary variables to 1.24% (i.e. 1.24%=2,019/162,816). Both decomposition and reduction techniques together can reduce the number of binary variables to 0.094% (i.e. 0.094%=153/162,816). It can be observed that both acceleration techniques can significantly reduce the size of the MIP model in the BE approach. In contrast, the reduction technique in the EP approach can only reduce the numbers of constraints and continuous variables. The number of binary variables remains 2,400 when the reduction technique is applied in the EP approach.

The performance of the MIP solver is not only related to the problem size, but also to the model itself. As shown in the last row of Table VI, the MIP models in the BE approach and the EP approach have similar sizes (i.e. around 400 constraints and 500 variables) when the two acceleration techniques are applied. However, the MIP solver has much better computational performance in the BE approach than that in the EP approach according to Table V. If only the decomposition technique is applied, the presolved MIP model has 14,401 constraints and 6,784 binary variables in the BE approach, which is much larger than the MIP model with 406 constraints and 100 binary variables in the EP approach. But the average solution time in the BE approach is still much less than that in the EP approach according to Table V. These observations indicate that the MIP solver has better computational performance for the models in the BE approach. It suggests that the cutting plane technique and other techniques in the modern MIP solver are more effective for the proposed model.

VI. CONCLUSION

In this paper, a novel BE approach to solve the max-min problem is proposed in the RSCUC framework. The non-convex max-min problem is reformulated as a MIP problem. The new reformulation is not dependent on the closed forms for the extreme points in uncertainty set. The solution quality of the max-min problem is observable and controllable in the proposed BE approach. To reduce the computation burden, two effective acceleration techniques are also proposed in this paper. The effectiveness and advantages are demonstrated in the case study with IEEE 118-Bus system.

The NP-hard max-min problem in the robust SCUC framework is notoriously hard to solve. The global optimality of the max-min problem is the most essential part in RSCUC because it represents the solution robustness. The BE approach proposed in this paper shows the good performance in the optimality as well the computation time. Furthermore, it is applicable when other uncertainty sets are adopted. It will be useful in the data-driven RSCUC which tries to overcome the conservativeness issue. If RSCUC is used for market clearing, the controllable and observable solution quality in the proposed BE approach has important implications, as different solutions may lead to various prices. It is an important future work.

It is also possible to further improve the computation performance with a hybrid solution approach combined with BE and MC/OA. The BE approach can be applied to check the global optimality and generate the new worst point after the RSCUC solution is converged with the MC/OA approach. The solution from the BE approach can also serve as a starting point in the MC/OA approach.

Another future work is to test the proposed BE approach on large-scale systems. Based on the results of a preliminary simulation study with the ISO-scale Polish system [27], the proposed BE approach is still tractable for solving the max-min problem. We also plan to work with several ISOs in the U.S. to test the proposed BE approach using the real data of their systems.

Appendix A
Detailed Formulation of (P) and $\mathcal{R}(\boldsymbol{\epsilon})$

$$\min_{(y,z,I,p)\in\mathcal{F}} \sum_t \sum_g C(p_{g,t}, I_{g,t}) \tag{33}$$

$$\text{s.t} \quad \sum_g p_{g,t} = \sum_m d_{m,t}, \forall t \tag{34}$$

$$-F_l \le \sum_m \Gamma_{l,m}\Big(\sum_{g\in\mathcal{G}(m)} p_{g,t} - d_{m,t}\Big) \le F_l, \forall l, t \tag{35}$$

$$I_{g,t}p_g^{\min} \le p_{g,t} \le I_{g,t}p_g^{\max}, \forall g, t \tag{36}$$

$$p_{g,t} - p_{g,(t-1)} \le r_g^u(1-y_{g,t}) + p_g^{\min} y_{g,t}, \forall g, t \tag{37}$$

$$-p_{g,t} + p_{g,(t-1)} \le r_g^d(1-z_{g,t}) + p_g^{\min} z_{g,t}, \forall g, t \tag{38}$$

$$\text{minimum on/off time limit,} \tag{39}$$

where $p_{g,t}$, $I_{g,t}$, $y_{g,t}$, and $z_{g,t}$ are unit dispatch, unit status, startup indicator, and shutdown indicator, respectively. r_g^u and r_g^d are unit ramping up and ramping down rates, respectively. In this paper, $\boldsymbol{x}$ denotes the binary variable vector including $I_{g,t}$, $y_{g,t}$, and $z_{g,t}$, and $\boldsymbol{p}$ denotes the dispatch vector. (34) represents the generation/load balance constraint; (35) represents the power flow constraint; (36) represents the minimum and maximum capacity constraints; (37)-(38) represent the ramping up and ramping down constraints, respectively. Constraints (34)-(39) are rewritten as

$$\boldsymbol{Ax} + \boldsymbol{Bp} \le \boldsymbol{b}.$$

The feasible set $\mathcal{F}$ is defined as

$$\mathcal{F} := \Big\{(y,z,I,p) : \forall \boldsymbol{\epsilon} \in \mathcal{U}, \exists \Delta \boldsymbol{p},$$

$$\sum_g \Big(p_{g,t} + \Delta p_{g,t}\Big) = \sum_m \Big(d_{m,t} + \epsilon_{m,t}\Big), \forall t \tag{40}$$

$$-F_l \le \sum_m \Gamma_m \Big(\sum_{g\in\mathcal{G}(m)} \Big(p_{g,t} + \Delta p_{g,t}\Big) - d_{m,t} - \epsilon_{m,t}\Big) \le F_l, \forall l, t \tag{41}$$

$$\underline{r}_{g,t}(\boldsymbol{x},\boldsymbol{p}) \le \Delta p_{g,t} \le \bar{r}_{g,t}(\boldsymbol{x},\boldsymbol{p}), \forall g, t\Big\} \tag{42}$$

where $\bar{r}_{g,t}(\boldsymbol{x},\boldsymbol{p})$ and $\underline{r}_{g,t}(\boldsymbol{x},\boldsymbol{p})$ are the upper bound and lower bound of $\Delta p_{g,t}$. Constraints (40)-(41) are rewritten as

$$\boldsymbol{D}(\boldsymbol{p} + \boldsymbol{\Delta p}) + \boldsymbol{E\epsilon} \le \boldsymbol{h}.$$

Constraint (42) is rewritten as

$$\boldsymbol{Fx} + \boldsymbol{Gp} + \boldsymbol{H\Delta p} \le \boldsymbol{g}.$$

$\mathcal{R}(\boldsymbol{\epsilon})$ is formulated as

$$\mathcal{R}(\boldsymbol{\epsilon}) := \Big\{(\boldsymbol{\Delta p}, \boldsymbol{s^{D+}}, \boldsymbol{s^{D-}}, \boldsymbol{s^{L+}}, \boldsymbol{s^{L-}}) : \tag{43}$$

$$\boldsymbol{s^{D+}}, \boldsymbol{s^{D-}}, \boldsymbol{s^{L+}}, \boldsymbol{s^{L-}} \ge \boldsymbol{0}$$

$$\sum_g \Big(p_{g,t} + \Delta p_{g,t}\Big) = \sum_m \Big(d_{m,t} + \epsilon_{m,t}\Big) + s_t^{D+} - s_t^{D-}, \forall t \tag{44}$$

$$p_{m,t}^{\text{inj}} = \sum_{g\in\mathcal{G}(m)} \Big(p_{g,t} + \Delta p_{g,t}\Big) - d_{m,t} - \epsilon_{m,t}, \forall m, t \tag{45}$$

$$-F_l \le \sum_m \Big(\Gamma_{l,m} p_{m,t}^{\text{inj}}\Big) + s_l^{L+} - s_l^{L-} \le F_l, \forall l, \forall t \tag{46}$$

$$\underline{r}_{g,t}(\boldsymbol{x},\boldsymbol{p}) \le \Delta p_{g,t} \le \bar{r}_{g,t}(\boldsymbol{x},\boldsymbol{p}), \forall g, t\Big\} \tag{47}$$

where (44) denotes the generation/load balance constraints, (45) defines the net power injection $p_{m,t}^{\text{inj}}$, (46) denotes the line capacity constraints, (47) denotes the limits of the unit generation adjustment $\Delta p_{g,t}$ as a function of given UC and ED as well as unit ramping rates and generation capacities.

Appendix B
Proof of Theorems 1 and 2

$\boldsymbol{\lambda}^\top \boldsymbol{E\epsilon}$ is approximated as

$$\boldsymbol{\lambda}^\top \boldsymbol{E\epsilon} = \boldsymbol{\lambda}^\top(\boldsymbol{q} + \underline{\boldsymbol{q}}) = \sum_i^{N_s} \lambda_i q_i + \boldsymbol{\lambda}^\top \underline{\boldsymbol{q}}$$

$$\approx \sum_i^{N_s} \sum_{k=0}^{K} 2^{-k} z_{i,k} q_i + \boldsymbol{\lambda}^\top \underline{\boldsymbol{q}}$$

Denote $\xi_{i,k} := z_{i,k} q_i$. We have

$$\xi_{i,k} = \begin{cases} q_i, & \text{if } z_{i,k} = 1, \quad (48) \\ 0, & \text{if } z_{i,k} = 0. \quad (49) \end{cases}$$

$\boldsymbol{\epsilon}$ is bounded according to the definition of $\mathcal{U}$. Hence, $\boldsymbol{E\epsilon}$ is also bounded. With (18), we also have $\boldsymbol{0} \le \boldsymbol{q} \le \bar{\boldsymbol{q}}$. Therefore, constraints (48)(49) are equivalent to the following constraints

$$\begin{cases} \xi_{i,k} \ge 0, \quad \xi_{i,k} \ge q_i - \bar{q}_i + \bar{q}_i z_{i,k} & (50) \\ \xi_{i,k} \le \bar{q}_i z_{i,k}, \quad \xi_{i,k} \le q_i & (51) \end{cases}$$

Furthermore, as (RP) is a maximization problem and the coefficients of $\xi_{i,k}$ are positive, the constraints (50) are redundant.

The feasible region of $\boldsymbol{\lambda}$ and $\boldsymbol{\mu}$ in (RP) remain the same, although (17) is introduced to linearize the bilinear term in the objective function. Then, we only need to consider the difference of the objective functions.

$$\begin{aligned}
&\left|\boldsymbol{\lambda}^\top \boldsymbol{E}\boldsymbol{\epsilon} - \left(\sum_{i}^{N_s}\sum_{k=0}^{K} 2^{-k} z_{i,k} q_i + \boldsymbol{\lambda}^\top \underline{\boldsymbol{q}}\right)\right| \\
=&\left|\sum_{i}^{N_s} \lambda_i q_i - \sum_{i}^{N_s}\sum_{k=0}^{K} 2^{-k} z_{i,k} q_i\right| \\
=&\left|\sum_{i}^{N_s} \left(\lambda_i - \sum_{k=0}^{K} 2^{-k} z_{i,k}\right) q_i\right| \\
\leq&\sum_{i}^{N_s} 2^{-K} \bar{q}_i
\end{aligned}$$

The first equality follows (18). With the upper bound of BE approximation $|\lambda_i - \sum_{k=0}^{K} 2^{-k} z_{i,k}| \leq 2^{-K}$, the inequality follows.

Appendix C
Proof of Theorem 3

The flow constraint for line l in the positive direction at t is inactive if line capacity F_l is greater than

$$\max\left\{\sum_m \Gamma_{l,m} p^{\text{inj}}_{m,t} : \sum_m p^{\text{inj}}_{m,t} = 0,\ \underline{p}^{\text{inj}}_{m,t} \leq p^{\text{inj}}_{m,t} \leq \bar{p}^{\text{inj}}_{m,t}\ \forall m\right\}.$$

With the introduction of $p^{\text{inj+}}_{m,t} := p^{\text{inj}}_{m,t} - \underline{p}^{\text{inj}}_{m,t}$, the above problem is reformulated as

$$\max\left\{\begin{aligned}\sum_m \Gamma_{l,m} p^{\text{inj+}}_{m,t} + f^{\text{vt}}_{l,t} : &\sum_m p^{\text{inj+}}_{m,t} = p^{\text{vt}}_t, \\ &0 \leq p^{\text{inj+}}_{m,t} \leq \bar{p}^{\text{inj+}}_{m,t}\ \forall m\end{aligned}\right\} \tag{52}$$

If (52) is feasible, there must exist an integer j satisfying (24). If the shift factors are ordered as (26), the optimal solution to (52) is

$$p^{\text{inj+}}_{m_n,t} = \begin{cases} \bar{p}^{\text{inj+}}_{m_n,t}, & n = 1, \cdots, j-1 \\ p^{\text{vt}}_t - \sum_{n=1}^{j-1} \bar{p}^{\text{inj+}}_{m_n,t}, & n = j \\ 0, & n = j+1, \cdots, N_d, \end{cases}$$

and the optimal value is

$$\begin{aligned}
&\sum_{n=1}^{j-1} \Gamma_{l,m_n} \bar{p}^{\text{inj+}}_{m_n,t} + \Gamma_{l,m_j}\left(p^{\text{vt}}_t - \sum_{n=1}^{j-1} \bar{p}^{\text{inj+}}_{m_n,t}\right) + f^{\text{vt}}_{l,t} \\
=&\sum_{n=1}^{j-1} (\Gamma_{l,m_n} - \Gamma_{l,m_j}) \bar{p}^{\text{inj+}}_{m_n,t} + \Gamma_{l,m_j} p^{\text{vt}}_t + f^{\text{vt}}_{l,t}.
\end{aligned}$$

Therefore, Theorem 3 is proved.

Appendix D
Proof of Theorem 4

From step 2 to step 5 in Algorithm 3, there are T max-min subproblems. In the first iteration from step 6 to step 15, there are T max-min subproblems. After the first iteration from step 6 to step 15, there is only one max-min subproblem, and $\sum_t v_t$ decreases by 1 each time. The maximal violation after step 5 is $\sum_t \Lambda_t - \Lambda$. The while loop ends until $\sum_t v_t = \Lambda$ after $\sum_t \Lambda_t - \Lambda$ iterations. Hence, the total number of max-min subproblem is $2T + \sum_t \Lambda_t - \Lambda$. In fact, if $\phi_t(v_t) = 0$, then $\phi_t(v_t - 1)$ must be 0. Hence, in this case, there is no need to solve another max-min subproblem to get the value of $\phi_t(v_t - 1)$.

Appendix E
Proof of Proposition 1

The max-min problem (USP) can also be reformulated as a bilinear programming problem according to the duality theory. Denote it as (UBP). Consider λ^{ud}_t as the dual variable for (21) and λ^d_t for (44). On a side note, (44) is expressed as two inequality constraints in (10c). Then the only difference between (BP) and (UBP) is that

$$-1 \leq \lambda^d_t \leq 1, \forall t \tag{53}$$

while λ^{ud}_t is unbounded. Hence, $\phi^u \geq \phi$ follows. When the optimal solution $(\boldsymbol{x^*}, \boldsymbol{p^*})$ to (P) is found, we have $\phi = \phi^u = 0$. It means $\boldsymbol{s^{D+}} = \boldsymbol{s^{D-}} = \boldsymbol{0}$. Therefore, adding constraint

$$-1 \leq \lambda^{ud}_t \leq 1, \forall t$$

in (UBP) does not alter the optimal solution.

Appendix F
Proof of Proposition 2

It is observed that $\Big\{\mathcal{V}_1(v_1), \cdots, \mathcal{V}_T(v_T) : \sum_t v_t \leq \Lambda, v_t \leq \Lambda_t, v_t \in \mathbb{Z}_+\Big\} = \mathcal{U}$. On the other hand, given $(\boldsymbol{x}, \boldsymbol{\epsilon})$, the inner problem in (SP) is time-decoupled. Therefore, the feasible region of (IP) and that of (SP) are the same. Hence, $\phi^{\text{IP}} = \phi$ and solution $\boldsymbol{\epsilon}_t(v^*_t)$ is a sub-vector of $\boldsymbol{\epsilon}^*$.

References

[1] X. Guan, P. B. Luh, H. Yan, and J. Amalfi, "An optimization-based method for unit commitment," *International Journal of Electrical Power & Energy Systems*, vol. 14, no. 1, pp. 9–17, 1992.

[2] M. Shahidehpour, H. Yamin, and Z. Li, *Market Operations in Electric Power Systems: Forecasting, Scheduling, and Risk Management*, 1st ed. Wiley-IEEE Press, 2002.

[3] Z. Li and M. Shahidehpour, "Security-constrained unit commitment for simultaneous clearing of energy and ancillary services markets," *IEEE Trans. Power Sys.*, vol. 20, no. 2, pp. 1079–1088, 2005.

[4] "Integration of wind into system dispatch," New York ISO, Tech. Rep., 2008.

[5] "Integration of renewable resources," California ISO, Tech. Rep., 2010.

[6] L. Wu, M. Shahidehpour, and T. Li, "Stochastic security-constrained unit commitment," *IEEE Trans. Power Sys.*, vol. 22, no. 2, pp. 800–811, 2007.

[7] J. Wang, A. J. Conejo, C. Wang, and J. Yan, "Smart grids, renewable energy integration, and climate change mitigation–future electric energy systems," *Applied Energy*, vol. 96, pp. 1–3, 2012.

[8] R. Jiang, J. Wang, and Y. Guan, "Robust unit commitment with wind power and pumped storage hydro," *IEEE Trans. Power Systems*, vol. 27, no. 2, pp. 800 – 810, 2012.

[9] D. Bertsimas, E. Litvinov, X. Sun, J. Zhao, and T. Zheng, "Adaptive robust optimization for the security constrained unit commitment problem," *IEEE Trans. Power Syst.*, vol. 28, no. 1, pp. 52–63, 2013.

[10] H. Ye and Z. Li, "Robust security-constrained unit commitment and dispatch with recourse cost requirement," *IEEE Trans. Power Sys.*, DOI: 10.1109/TPWRS.2015.2493162.

[11] R. Jiang, M. Zhang, G. Li, and Y. Guan, "Two-stage network constrained robust unit commitment problem," *European Journal of Operational Research*, vol. 234, no. 3, pp. 751 – 762, 2014.

[12] C. Zhao and Y. Guan, "Unified stochastic and robust unit commitment," *IEEE Trans. Power Sys.*, vol. 28, no. 3, pp. 3353–3361, 2013.

[13] R. Wiser and M. Bolinger, "2011 wind technologies market report," Lawrence Berkeley National Laboratory, Tech. Rep., 2012.

[14] A. Nahapetyan, "Bilinear programming," Tech. Rep., 2007. [Online]. Available: http://plaza.ufl.edu/artyom/Papers/BilinerProgram.pdf

[15] B. Zeng and L. Zhao, "Solving two-stage robust optimization problems using a column-and-constraint generation method," *Operations Research Letters*, vol. 41, no. 5, pp. 457–461, sep 2013.

[16] H. Ye and Z. Li, "Robust security-constrained unit commitment with recourse cost requirement," in *Power Energy Society General Meeting, 2015 IEEE*, July 2015, pp. 1–5.

[17] A. Ben-Tal, A. Goryashko, E. Guslitzer, and A. Nemirovski, "Adjustable robust solutions of uncertain linear programs," *Math. Program., Ser. A*, vol. 99, no. 2, pp. 351–376, Mar. 2004.

[18] J. Warrington, P. Goulart, S. Mariethoz, and M. Morari, "Policy-based reserves for power systems," *IEEE Trans. Power Sys.*, vol. 28, no. 4, pp. 4427–4437, 2013.

[19] R. A. Jabr, "Adjustable robust OPF with renewable energy sources," *IEEE Trans. Power Sys.*, vol. 28, no. 4, pp. 4742–4751, 2013.

[20] Z. Li, W. Wu, B. Zhang, and B. Wang, "Adjustable robust real-time power dispatch with large-scale wind power integration," *IEEE Transactions on Sustainable Energy*, vol. PP, no. 99, pp. 1–12, 2015.

[21] X. Guan, Q. Zhai, and A. Papalexopoulos, "Optimization based methods for unit commitment: Lagrangian relaxation versus general mixed integer programming," in *Power Engineering Society General Meeting, 2003, IEEE*, July 2003.

[22] R. Chandrasekaran, S. N. Kabadi, and K. G. Murthy, "Some NP-complete problems in linear programming," *Oper. Res. Lett.*, vol. 1, no. 3, pp. 101–104, jul 1982.

[23] A. Gupte, S. Ahmed, M. S. Cheon, and S. Dey, "Solving mixed integer bilinear problems using MILP formulations," *SIAM Journal on Optimization*, vol. 23, no. 2, pp. 721–744, 2013.

[24] H. Ye and Z. Li, "Necessary conditions of line congestions in uncertainty accommodation," *IEEE Trans. Power Systems*, DOI:10.1109/TPWRS.2015.2508643.

[25] Q. Zhai, X. Guan, J. Cheng, and H. Wu, "Fast identification of inactive security constraints in SCUC problems," *IEEE Trans. Power Sys.*, vol. 25, no. 4, pp. 1946–1954, 2010.

[26] I. Gurobi Optimization, *Gurobi Optimizer Reference Manual*, 2014. [Online]. Available: http://www.gurobi.com

[27] R. Zimmerman, C. Murillo-Sanchez, and R. Thomas, "Matpower: Steady-state operations, planning, and analysis tools for power systems research and education," *IEEE Trans. Power Sys.*, vol. 26, no. 1, pp. 12–19, Feb 2011.

Hongxing Ye (S'14-m'16) received his B.S. degree in Information Engineering, in 2007, and M.S. degree in Systems Engineering, in 2011, both from Xi'an Jiaotong University, China, and the Ph.D. degree in Electrical Engineering from the Illinois Institute of Technology, Chicago in 2016. His research interests include large-scale optimization in power systems, electricity market, renewable integration, and cyber-physical system security in smart grid. He is "Outstanding Reviewer" for IEEE Transactions on Power Systems and IEEE Transactions on Sustainable Energy in 2015. He received Sigma Xi Research Excellence Award at Illinois Institute of Technology in 2016.

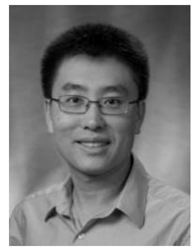

Jianhui Wang (M07-SM12) received the Ph.D. degree in electrical engineering from Illinois Institute of Technology, Chicago, IL, USA, in 2007. Presently, he is the Section Lead for Advanced Power Grid Modeling at the Energy Systems Division at Argonne National Laboratory, Argonne, IL, USA. Dr. Wang is the secretary of the IEEE Power & Energy Society (PES) Power System Operations Committee. He is an associate editor of Journal of Energy Engineering and an editorial board member of Applied Energy. He is also an affiliate professor at Auburn University and an adjunct professor at University of Notre Dame. He has held visiting positions in Europe, Australia and Hong Kong including a VELUX Visiting Professorship at the Technical University of Denmark (DTU). Dr. Wang is the Editor-in-Chief of the IEEE Transactions on Smart Grid and an IEEE PES Distinguished Lecturer. He is also the recipient of the IEEE PES Power System Operation Committee Prize Paper Award in 2015.

Zuyi Li (SM'09) received the B.S. degree from Shanghai Jiaotong University, Shanghai, China, in 1995, the M.S. degree from Tsinghua University, Beijing, China, in 1998, and the Ph.D. degree from the Illinois Institute of Technology (IIT), Chicago, in 2002, all in electrical engineering. Presently, he is a Professor in the Electrical and Computer Engineering Department at IIT. His research interests include economic and secure operation of electric power systems, cyber security in smart grid, renewable energy integration, electric demand management of data centers, and power system protection.